Figur 2E

Supporting Information for Szyperski *et al.* (2002) *Proc. Natl. Acad. Sci. USA* **99** (12), 8009–8014. (10.1073/pnas.122224599).

Supporting Figure 8

Fig. 8. Experimental scheme for the 3D $H^{a/b}C^{a/b}COHA$ experiment. Rectangular 90° and 180° pulses are indicated by thin and thick vertical bars, respectively, and phases are indicated above the pulses. Where no rf phase is marked, the pulse is applied along x. The scaling factor k for the ^1H chemical shift evolution during t_1 is set to 1.0. The high power 90° pulse lengths were: 5.9 ms for ^1H, 15.4 ms for ^{13}C, and 38.2 ms for ^{15}N. The 90° and 180° pulse lengths of $^{13}C^{a/b}$ were adjusted to 47.4 and 42.4 ms, respectively, to minimize perturbation of ^{13}CO spins. A 200-ms 180° pulse with SEDUCE profile is used to selectively invert ^{13}CO magnetization prior to the start of t_1. The 90° and 180° pulses employed for excitation of ^{13}CO and subsequent magnetization transfer back to $^{13}C^a$ are of rectangular shape and 52 and 103 ms duration, respectively. The length of the spin-lock purge pulses SL_x and SL_y are 2.5 and 1 ms, respectively. WALTZ16 is employed to decouple ^1H (rf field strength = 9.2 kHz) during the heteronuclear magnetization transfers, and for decoupling of ^{15}N (rf = 1.78 kHz) during acquisition. GARP is used for decoupling of $^{13}C^a$ (rf = 2.5 kHz). The ^1H rf carrier is placed at the position of the solvent line at 0 ppm before the start of the first semiconstant time ^1H evolution period and then switched to the water line at 4.78 ppm after the second 90° ^1H pulse. Initially, the ^{13}C and ^{15}N rf carriers are set to 43 and 120.9 ppm, respectively. The duration and strengths of the pulsed z-field gradients (PFGs) are: G1 = G2 (100 ms, 15 G/ cm); G3 (2 ms, 25 G/cm); G4 (100 ms, 10 G/cm); G5 (1 ms, 27 G/cm); G6 (3 ms, 30 G/cm); G7 (1.3 ms, 20 G/cm); G8 (130 ms, 14 G/cm). All PFG pulses are of rectangular shape. A recovery delay of at least 100 ms duration is inserted between a PFG pulse and an rf pulse. The delays are: t_1 = 800 ms, t_2 = 2.8 ms, t_3 = 3.6 ms, t_4 = 6.5 ms, t_5 = 1.8 ms, t_6 = 1 ms, t_7 = 2.8 ms, t_8 = 3.6 ms. ^1H-frequency labeling is achieved in a semi constant-time fashion with t_1^a (0) = 1.7 ms, t_1^b (0) = 1 ms, t_1^c (0) = 1.701 ms, Dt_1^a = 33.3 ms, Dt_1^b = 19.3 ms, and Dt_1^c = -14 ms. Hence, the fractional increase of the semi constant-time period with t_1 equals to $l = 1 + Dt_1^c / Dt_1^a = 0.58$. Phase cycling: $f_1 = x$; $f_x = x, -x$; $f_3 = x, -x, x, -x$; $f_4 = x$; f_5(receiver) = $x, -x$. Quadrature detection in t_1($^{13}C/^1H$) and t_2(^{15}N) is accomplished by altering the phases f_2 and f_4, respectively, according to States-TPPI. Water suppression is accomplished by coherence pathway rejection using spin-lock purge pulses and pulsed field z-gradients. For acquisition of central peaks derived from ^{13}C steady state magnetization, a second data set with f_1 = -x is collected. The sum and the difference of the two resulting data sets generate subspectra II and I, respectively, containing the central peaks and peak pairs.

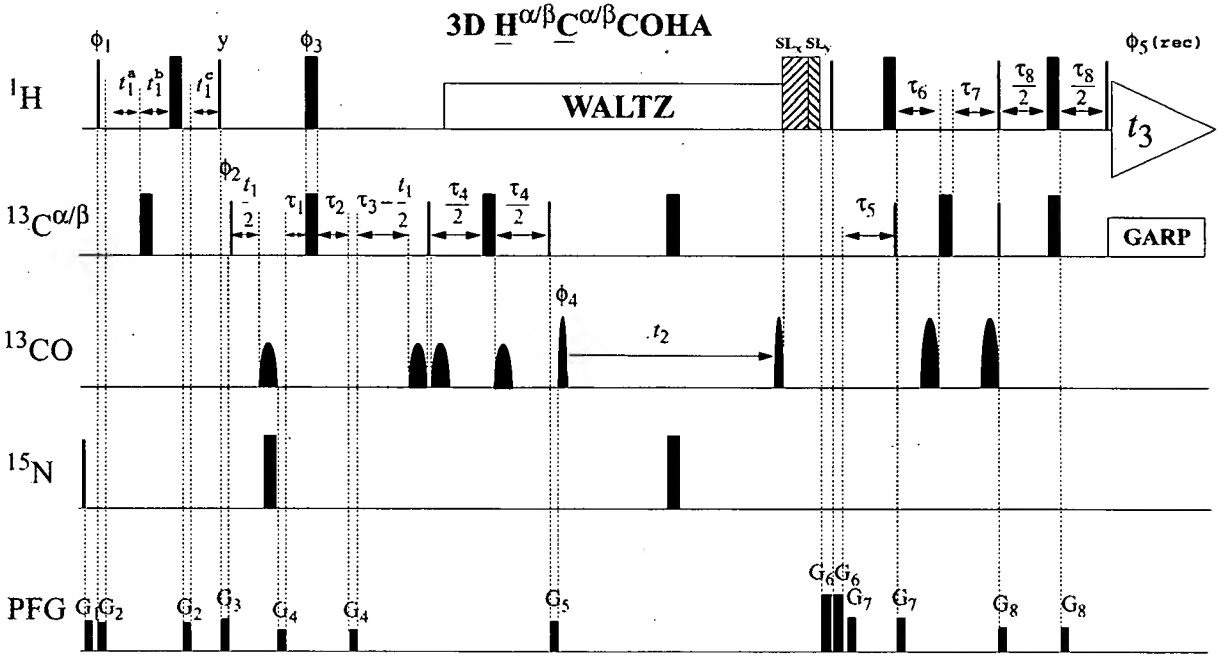
3D H^α/βC^α/βCOHA
ϕ1
y
ϕ3
SL_x SL_y
ϕ5(rec)
1H
WALTZ
τ6
τ7
τ8/2
τ8/2
t3
ϕ2
t1/2
τ1
τ2
τ3 − t1/2
τ4/2
τ4/2
τ5
13Cα/β
GARP
ϕ4
13CO
t2
15N
PFG
G1 G2
G2
G3
G4
G4
G5
G6 G6
G7
G7
G8
G8

Figure 8